UNIVERSITY OF TURKU

Hydrogen embrittlement susceptibility of selective laser melted, and post-heat treated AISI 316 L and Inconel 718 steels

Materials engineering

Bachelor's thesis

Author:

Mirka Mettinen

1.4.2024

Turku

Bachelor's thesis

Subject: Materials engineering
Author: Mirka Mettinen
Title: Hydrogen embrittlement susceptibility of selective laser melted, and post-heat treated AISI 316 L and Inconel 718 steels
Supervisor: Dr Emilia Palo
Number of pages: 30
Date: 1.4.2024

Abstract

Laser powder bed fusion is one of many additive manufacturing techniques where specimen is fabricated layer by layer via melting powder selectively with laser beam. Additive manufacturing provides benefits including reduced material needs and waste, closer localization of spare part production and suppressed warehouses. However, the microstructural features formed during the manufacturing process differs from a conventionally produced counterparts leading to modified mechanical properties and performance in various circumstances. Hydrogen embrittlement is a phenomenon that embrittles metals, where hydrogen absorbs into the lattice through high pressure gas environment or electrochemical reaction causing decrease in toughness. It is extensively studied phenomena in metal materials, but the mechanisms and factors enhancing brittleness are further uncertain. Thus, thorough research of hydrogen embrittlement behaviour in additively manufactured metals is necessary to prevent premature failures causing dreadful accidents. The aim of the thesis is to raise awareness of the current research findings promoting hydrogen embrittlement in selective laser melted AISI 316 L and Inconel 718 steels, involving microstructural features, fracture mechanisms and mechanical properties. Both steels manufactured by selective laser melting are subjected to several post-heat treatments and compared to each other and their conventionally produced counterparts, to discuss the most compatible post-processed steel for hydrogen environment.

The selective laser melting reduces hydrogen embrittlement susceptibility in both materials which can be explained by the unique microstructure formed during the manufacturing process. Moreover, the properties and hydrogen embrittlement vulnerability were able to be altered with post-heat treatments. Hot isotopic pressing and heat treatment without polishing procedures of AISI 316 L exhibited the highest resistance with a minimal brittleness. For one's part, homogenization plus one aging treatment showed the lowest hydrogen embrittlement behaviour in Inconel 718, yet it does not compare to AISI 316 L. The grain and cell boundaries acted as a hydrogen accumulation and diffusion paths in both steels, but the primary factors enhancing hydrogen embrittlement were separate. The focus in AISI 316 L was dislocation structure and density while the detrimental features of Inconel 718 were precipitants γ', γ'', δ and Laves phases. Based on the research results, AISI 316 L is more compatible steel for hydrogen environment, but the hot isotopic pressing treatment caused the lowest yield and tensile strengths, and the absence of surface polishing could be problematic in the place of use. Hydrogen embrittlement behavior of selective laser melted steels requires further studies to achieve thorough understanding of the phenomenon where the conclusions of the thesis provide potential investigation paths.

Keywords: Additive manufacturing, selective laser melting, hydrogen embrittlement, post-heat treatment

Kandidaatin tutkielma

Oppiaine: Materiaalitekniikka
Kirjoittaja: Mirka Mettinen
Otsikko: Vetyhauraus jauhepetisulatetuilla sekä lämpökäsitellyillä AISI 316 L- ja Inconel 718 -teräksillä
Tarkastaja: FT Emilia Palo
Sivujen määrä: 30
Päivämäärä: 1.4.2024

Tiivistelmä

Materiaalia lisäävä valmistus on kasvava tulostustekniikka, jossa materiaalia lisätään kerros kerrokselta. Valmistustekniikalla on useita hyötyjä, kuten pienempi materiaali- ja varastotilojen tarve sekä tuotantojäte ja varaosatuotannon mahdollinen uudelleensijoitus lähemmäksi. Mikrorakenteelliset ominaisuudet kuitenkin eroavat tavanomaisella tavalla valmistetuista vastineista, mikä johtaa erilaisiin mekaanisiin ominaisuuksiin sekä suorituskykyyn vaihtelevissa olosuhteissa. Vetyhauraus on metalleja haurastuttava ilmiö, jossa vetyatomi absorboituu metallihilaan korkeapaineisessa vetykaasuympäristössä tai sähkökemiallisen reaktion myötä ja aiheuttaa sitkeyden heikkenemistä sekä hauraan murtumaan. Metallien vetyhaurastumista on laajalti tutkittu, mutta haurautta edistävät mekanismit ja tekijät ovat edelleen kiistanalaisia. Täten tulostustekniikalla valmistetun metallin perusteellinen vetyhaurauskäyttäytymisen tutkiminen on välttämätöntä ennenaikaisten murtumien estämiseksi. Opinnäytetyön tavoitteena on lisätä tietoisuutta ajankohtaisista tutkimustuloksista, jotka edistävät jauhepetisulatettujen AISI 316 L- ja Inconel 718 -terästen vetyhaurautta käyttämällä jauheen sulatustekniikkana kuitulaseria. Ilmiötä tutkitaan murtumismekanismien ja mikrorakenteellisten sekä mekaanisten ominaisuuksien näkökulmasta. Molemmille teräsmateriaaleille tehdään useita erilaisia jälkikäsittelyjä, joiden ominaisuuksia vertaillaan keskenään sekä tavanomaisella tavalla valmistettuihin vastineisiin. Tulosten perusteella pohditaan vety-ympäristöön yhteensopivampaa terästä ja lämpökäsittelytekniikkaa.

Materiaalia lisäävä valmistus vähensi vetyhaurausherkkyyttä molemmissa materiaaleissa, mikä voidaan perustella jauhepetisulatuksen aikana muodostuneen ainutlaatuisen mikrorakenteen avulla. Lisäksi tutkittavien teräksien ominaisuuksia sekä vetyhaurausherkkyyttä oli mahdollista muokata lämpökäsittelyiden avulla. Suurin vetyhaurauden kestävyys havaittiin AISI 316 L teräksellä kuuman isostaattisen puristuskäsittelyn ja pintakäsittelemättömän lämpökäsittelyn jälkeen. Puolestaan Inconel 718:n yhden ikäännyttämisvaiheen sisältävä homogenisointikäsittely osoitti suurinta vetyhaurauskestävyyttä, mutta se ei kuitenkaan ole verrattavissa AISI 316 L teräkseen. Mikrorakenteen rae- ja solurajat toimivat vedyn kasaantumis- ja diffuusioasemina, mutta ensisijaiset vetyhaurautta edistävät tekijät erosivat tutkittavien teräksien välillä. Haitalliset ominaisuudet AISI 316 L teräksessä olivat dislokaatiorakenne sekä -tiheys ja Inconel 718: ssa γ'-, γ''-, δ -saostumat ja Laves -faasit. Tulosten perusteella voidaan todeta, että AISI 316 L on ominaisuuksiltaan suotuisampi vaihtoehto, mutta kuuman isostaattisen puristuskäsitellyn teräksen myötö- ja vetolujuus olivat tutkimuksien heikoimpia sekä pintakäsittelemättömän teräksen pinnankarheus voi aiheuttaa ongelmia, jotka tulee ottaa huomioon käyttökohteen vaatimuksia ajatellen. Jauhepetisulatettujen metallien vetyhauras vaatii yhä syvempää tutkimusta ilmiön perusteellisen ymmärryksen saavuttamiseksi, mihin opinnäytetyö antaa potentiaalisia tutkimussuuntia.

Avainsanat: Materiaalia lisäävä valmistus, materiaalin sulatus kuitulaserilla, vetyhauraus, lämpökäsittely

Table of contents

Abbreviations

AM	Additive manufacturing
L-PBF	Laser powder bed fusion
SLM	Selective laser melting
HE	Hydrogen embrittlement
CAD	Computer aided design
SSTR	Slow strain rate tensile test
EBSD	Electron backscatter diffraction
ECCI	Electron channelling contrast imaging
SEM	Scanning electron microscope
FCC	Face-centred cubic
HELP	Hydrogen enhanced local plasticity
HEDE	Hydrogen enhanced decohesion
IG	Intergranular
TG	Transgranular
HAC	Hydrogen assisted cracking
SIM	Strain-induced martensite
RA	Reduction of area
EF	Elongation to fracture
AH	Age-hardening
SAT	Solution aging treatment
ST	Solution treatment
HA1	Homogenization + aging treatment
HA2	Homogenization + double aging treatment
DA	Direct aging
H1, H2	Heat treatment
ANN	Annealing treatment
HIP	Hot isostatic pressing
CW	Hot isostatic pressing and pre-straining at 30 % elongation
HP	Heat treatment with polishing stage

1 Introduction

Additive manufacturing (AM) is a continuously growing worldwide field making a revolution to the production industry [1]. AM provides plenty of advantages including reduced material needs and waste, manufacturing of complex geometries, and closer localization of spare part production. Despite that hydrogen embrittlement (HE) is widely examined phenomena, the mechanisms, and factors behind it are still debatable. The microstructure of AM products varies from its conventionally produced counterparts leading to modified mechanical properties and hydrogen embrittlement behaviour. Hydrogen embrittlement weaken mechanical properties of metals causing abruptly catastrophic accidents without any warning signs in advance. This raises the necessity to investigate hydrogen embrittlement behaviour thoroughly in additively manufactured metal materials.

AISI 316 L and Inconel 718 steels are used in versatile applications for example in valves, hydrogen energy systems, automotive and aerospace industries. AISI 316 L is an austenitic stainless-steel containing ~67% of iron, 16.5-18.5% of chromium, 10-13% of nickel, and smaller amounts of other elements such as molybdenum. It has exceptional corrosion and acid resistance, good ductility properties but low yield and tensile strengths due to soft face-centred cubic (FCC) austenite phase. In turn, Inconel 718 is a nickel-chromium alloy that contains 50-55% of nickel, 17-21% of chromium, and smaller concentrations of other elements including iron, molybdenum and niobium [2]. Inconel 718 is recognized for its excellent mechanical strength properties achieved by the formation of precipitates during aging treatment. Along with the high strength properties, it has an outstanding strength-to-weight ratio with good toughness, corrosion, and temperature resistance but its ductility features do not compare to AISI 316 L. [3–5]

The effect of hydrogen to the microstructures, fracture mechanisms and mechanical properties of additively manufactured and post-heat treated AISI 316 L and Inconel 718 steels are controversial requiring further examination. Multiple hydrogen trapping sites, diffusion paths and fracture mechanisms have been detected that interplays together making it difficult to thoroughly understand the contribution of separate features leading to HE. The aim of the thesis is to gain knowledge of predisposing factors leading to hydrogen embrittlement of selective laser melted (SLM) and post-heat treated AISI 316 L and Inconel 718 steels. Both steels are exposed to multiple post-heat treatments which are compared to each other and their

conventionally produced counterparts to discuss the most compatible steel and post-heat treatment for hydrogen environment. This thesis aims to answer the following questions:

- Does laser powder bed fusion promote hydrogen embrittlement susceptibility?
- Is AISI 316 L or Inconel 718 steel more suitable for hydrogen environment?
- Which post-heat treatment technique indicate the highest hydrogen embrittlement resistance?

The additive manufacturing technique in interest is selective laser melting which is a subclass of the laser powder bed fusion (L-PBF). Several investigation methods were used in the literature to determine the properties of steels. Slow strain rate tensile (SSTR) test machine was utilized to quantify the reduction of area (RA), elongation to fracture (EF), yield, and tensile strengths. The microstructure evolutions and crack characteristics were determined with combined electron backscatter diffraction (EBSD) and electron channelling contrast imaging (ECCI). Scanning electron microscope (SEM) device was used to grain structure characterizations. Either electrochemical or high-pressure gaseous hydrogen charging was executed to the specimens with various treatment times, pressures, temperatures, solutions, and current densities which may have led to different hydrogen concentrations inside the materials and cause debatable results. However, the research results indicate hydrogen embrittlement mechanisms and enhancing factors while giving the direction for further investigations. [6,7]

2 Selective laser melting

Additive manufacturing is the opposite technique when compared to conventional production because it is based on adding material layer by layer, instead of removing with machining tools. The product is modelled with computer aided design (CAD) and fabricated by using three-dimensional printer. A support structure modelled by CAD is usually required during printing process and removed afterwards because the product cannot be manufactured on top of nothing. AM allows the production of complex geometries, for example internal cavities which are impossible to achieve by conventional methods. Spare part production can be re-located closer, and warehouses can be suppressed by digitalizing spare parts and produced only when needed on the site. In addition, additive manufacturing decreases the material needs and waste which is beneficial when thinking responsible consumption and sustainability. [8]

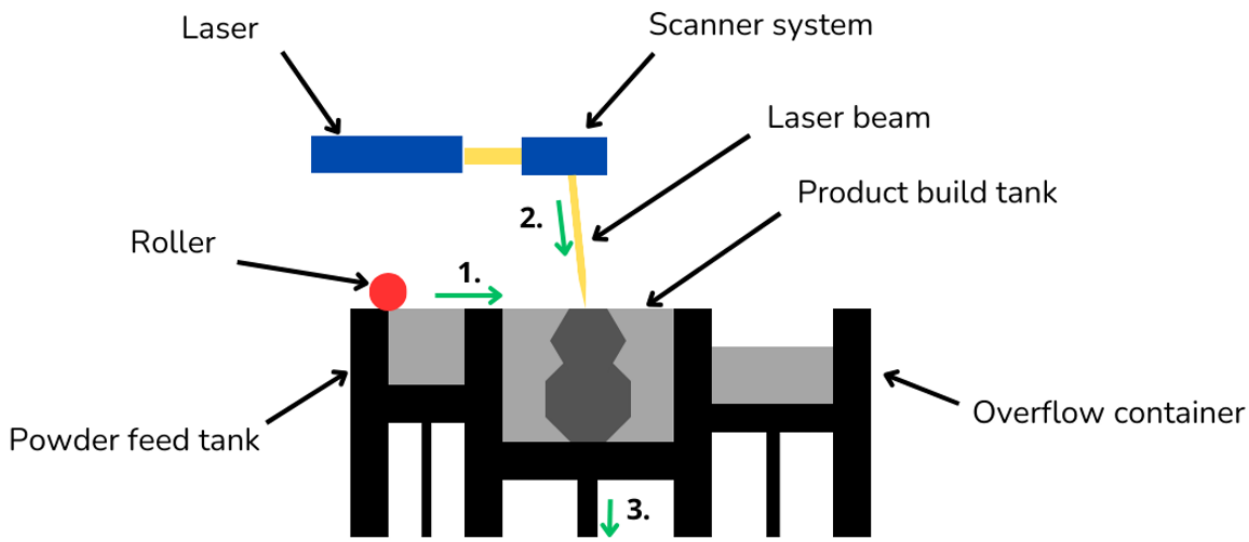

Figure 1. The selective laser melting device

Laser powder bed fusion is one of many but most used additive manufacturing technique for metals and the device includes a powder feed tank, a roller, a product build tank, an overflow container, and an energy source which are simplified in Figure 1. The selective laser melting technique is considered in the thesis meaning that the energy source used is a laser beam. The SLM device includes multiple process parameters which can be modified to achieve different

outcomes, for instance layer thickness, powder size, building chamber atmosphere, hatch spacing, laser power and scan speed [9,10]. However, the focus in the thesis is not the process parameters and they will not be discussed more closely.

2.1 The process of selective laser melting

The selective laser melting process begins with modelling the desirable product with a computer aided design software. The complete CAD file is then sliced into thin layers which is the thickness of each layer melted, and next the file is converted to a form that three-dimensional printer understands. The SLM process can be divided coarsely into three phases presented by the green arrows in Figure 1. The green arrow 1. indicates the first step which is relocating the powder from the powder feed tank to the product build tank by using a roller and spare powder is transferred to the overflow container where it can be reused. After a thin layer of powder is placed in the product build tank, the laser selectively fuses the powder together followed by rapid cooling pointed by the arrow 2. Lastly, the green arrow 3. expresses the third step where the product build tank is lowered down by the thickness of the layer and the exact same process is repeated until complete product. The product build tank is provided with an inert gas to prevent oxide layer formation on the surface of the specimen during the process. [11]

2.2 Metallurgical defects formed by selective laser melting

Numerous metallurgical defects are usually present after SLM and the defect formation varies between materials and selected process parameters [12]. Common defects formed during L-PBF are porosity, balling, incomplete fusion holes, surface roughness, voids, cracks, residual stress and melt pool boundaries. Hydrogen atoms can be trapped in these defects leading to diffusion and solution into the metal causing decreased mechanical properties [13]. Nevertheless, studies have suggested that the primary hydrogen embrittlement factors of AISI 316 L or Inconel 718 are not the defects which can be also suppressed by modifying the process parameters and via post-heat treatments. [6,14]

3 Hydrogen embrittlement

Hydrogen is the smallest atom in the nature that can be absorbed into metals during manufacturing process and in application via electrochemical reaction or high-pressure hydrogen gaseous environment. Absorbed hydrogen atoms are transported through interstitials lattice sites and trapped in various locations depending on the microstructure leading to accumulation in critical places [15–17]. Hydrogen causes detrimental behavior in metals by lowering mechanical properties such as tensile and yield strengths, fracture toughness along with changing the fracture mechanism from ductile to brittle known as hydrogen embrittlement. Moreover, HE enhances subcritical crack growth and fracture initiation through various mechanism leading to disastrous premature failure, possibly without any signs beforehand. [18]

Hydrogen can be trapped in multiple locations of the lattice and these trapping sites are divided into two main groups based on the activation energies ascribed as reversible and irreversible traps. The activation energy for irreversible trap is higher than 60 kJ/mol preventing hydrogen to escape at moderate temperature. For one's part, the activation energy of reversible trap is lower than 60 kJ/mol and thus, hydrogen can be escaped. The irreversible traps of the lattice are defined to be carbides, inclusions, and incoherent precipitates. The reversible hydrogen trapping sites, such as interstitial sites, dislocations, grain boundaries and coherent precipitants are suggested to primarily cause HE. The most detrimental hydrogen traps for AISI 316 L and Inconel 718 steels are precipitants, grain boundaries and dislocations which indeed are reversible traps. [17]

3.1 The fracture mechanisms of AISI 316 L and Inconel 718

The fracture mechanisms caused by hydrogen embrittlement have been studied extensively and two mechanisms have risen above others, which are hydrogen enhanced local plasticity (HELP) and hydrogen enhanced decohesion (HEDE). In HELP mechanism, hydrogen accelerates dislocation mobility and reduces the interplay between dislocations causing an increase in local plasticity and a decrease in shear stress. Shear stress enhances void formation which can coalesce along slip planes. Dislocation pile-ups on cell or grain boundaries are formed due to increased dislocation mobility leading to crack nucleation, propagation and lastly, premature fracture. In addition, HELP mechanism can decrease the fatigue of material plastic strain capacity causing a fracture. Hydrogen enhanced local plasticity can be observed by the lower yield strength, increased dislocation mobility and localized slip bands near the crack tips. In

turn, HEDE changes the fracture mode from ductile to cleavage-like failure by hydrogen accumulation at grain boundaries causing crystal lattice to expand and the lower atomic bond energy. Deteriorated atomic bond decreases the energy needed for crack propagation leading to brittle fracture. Intergranular (IG) and transgranular (TG) are the fracture propagation mechanisms where IG advances cracking along the grain boundaries and TG within grains. [16,18,19]

3.2 Hydrogen embrittlement index

Hydrogen embrittlement index (HEI) is a percentage value used to quantify materials susceptibility to hydrogen embrittlement. Various materials or post-heat treatments can be compared where higher HEI means increased susceptibility to hydrogen embrittlement. There are several equations used for calculating HEI index and the most sufficient equation is decided based on the material in question. The hydrogen embrittlement index can be determined by measuring elongation to failure, tensile strength, fracture strength, reduction of area and uniform plasticity before and after hydrogen charging [7,14,20,21]. The susceptibility of HE for Inconel 718 is quantified by measuring the decrease in elongation to fracture value and calculated by using Equation 1. where $TEl_{with\ H}$ is the elongation of hydrogen charged specimen and $TEl_{without\ H}$ of non-charged specimen. [14]

$$HEI\ \% = (1 - \frac{TEl_{with\ H}}{TEl_{without\ H}}) \cdot 100 \quad (1)$$

For AISI 316 L the HEI index is calculated mostly by using Equation 2. owing to the notable ductility feature pre and post hydrogen charging [6]. However, all studies of AISI 316 L did not measure the reduction of area value and in that case, the index is calculated by using Equation 1. In Equation 2, RA_A is the reduction of area of non-charged specimen and RA_H is correspondingly of hydrogen charged specimen.

$$HEI\ \% = (\frac{RA_A - RA_H}{RA_A}) \cdot 100 \quad (2)$$

4 Conventionally manufactured AISI 316 L and Inconel 718 steels

4.1 AISI 316 L

The influence of hydrogen in conventionally produced AISI 316 L steel is considered in this section and used to compare microstructural features, fracture mechanisms and mechanical properties to SLM counterparts. Annealing treatment was executed in the conventionally manufactured specimen which is indicated with initials CM. In its annealed state, CM specimen exhibited austenite microstructure with equiaxed grains, annealing twins and, ferrite stringers along the rolling direction and no martensite phase which is common for the material. The lattice included defects like voids but the volume of these along with other defects was much lower when compared to additively manufactured products. [6,22]

Strain induced martensite (SIM), especially α'-martensite is in the key role of hydrogen embrittlement of AISI 316 L because SIM acts as a diffusion path for hydrogen. Martensite formation is initiated by stress state, strain rate and temperature along with increasing hydrogen concentration and it varies between material's weight percent compositions. SIM formation can be predicted by using a Md_{30} formula where chemical compositions of the material are considered, and the results are expressed as a temperature where 30 % true tensile strain causes 50 % change from austenite to martensite phase. Based on the Md_{30}, the conventionally produced specimen is more prone to change from austenite to martensite phase than SLM counterparts which is suggested to be due to different microstructural features. [23]

Clear signs of hydrogen assisted cracking (HAC) were present on the fracture surface of the specimen which was proposed to play a big role of explaining the various behaviors in the presence of hydrogen. Dislocation pile-ups formed along grain boundaries during deformation caused stress concentrations leading to HAC initiation. Hydrogen enhanced α'-martensite formation, deformation twinning, planar deformation, and reduced stacking fault energy causing hydrogen assisted cracking [23]. Yield and tensile strengths remained the same or slightly increased in the presence of hydrogen and the measured values after hydrogen charging from two separate studies were 340, 690 MPa and 241.5, 621 MPa. The divergence between these values can be explained by the different charging times, pressures, and temperatures. In contrast, the elongation to fracture and reduction of area were decreased from 71.8 % to 60.5 % and 86.4 % to 56.6 % and in the other research the RA changed from 82 % to 57 % [6,24]. HEI values were calculated by using Equation 2. and the results were 34.5 % and 30.5 %

indicating that the ductility properties of AISI 316 L steel are notable decreased in the presence of hydrogen.

4.2 Inconel 718

The microstructural features and hydrogen assisted cracking in conventionally produced Inconel 718 are discussed briefly in this section and used as a comparison for determining the possibilities of using SLM products in hydrogen environment. Post-heat treatment technique investigated for Inconel 718 was age-hardening which was executed at 780 °C for 8 hours (AH1) and at 782 °C for 6.5 hours (AH2). Age-hardened Inconel 718 specimen exhibited austenite equiaxed grains including annealing twins, primary carbonitrides and precipitants such as γ′, γ′′ and δ formed during aging treatment which are common for the material. Precipitation free areas were found along the grain boundaries due to depletion of Nb. [25]

The fracture surface of hydrogen charged specimen was observed to be both ductile and brittle with quasi-cleavage fracture. Ductile fracture mode was detected mostly in the center of the specimen and brittle on the edges indicating that hydrogen affected mainly on the edges. Intergranular and transgranular crack propagation was found in brittle regions initiated by HELP and HEDE. IG cracking was noted in grain boundary triple junctions between grain boundaries and γ′-, γ′′- and δ -phases while TG crack propagation was observed in ridges, steps, and river patterns. Moreover, dislocation slips occurred in specific slip planes and nanovoids were observed along slip line intersections. HELP mechanism resulted shear localization areas along slip lines causing quasi-cleavage failure on these regions. It is discussed that hydrogen stabilizes edge component of mixed dislocations and decreases the stacking fault energy leading to enhanced slip planarity over cross slip. Hydrogen accumulation due to stress localization during deformation caused HEDE mechanism by reducing bonding strength between precipitants and grain boundaries. [25,26]

The elongation to fracture was decreased in the presence of hydrogen causing reduction in tensile strength but yield strength was not notable affected. The measured yield and tensile strengths of AH1 were 1000, 1050 MPa and for AH2 specimen 670, 850 MPa. Owing to the longer aging treatment and shorter charging time, AH1 had higher yield and tensile strength properties which is commonly observed in Inconel 718 steels. The correlation between hydrogen charging time, increased brittle depth and decreased elongation to fracture was clearly noted indicating susceptibility to HE. Four hour charging time led to decrease in EF from 45 % to 12 % in AH1 specimen and in turn, AH2 specimen without hydrogen was measured 27.6 %,

7.5 % with 20 hours of charging time and only 2.06 % with 120 hours [25]. Hydrogen embrittlement index values for both specimens were calculated by using Equation 1. and the results were 73.3 % for AH1, 72.8 % for AH2 with 20 hours of charging and 92.5 % for 120 hours. Interestingly, the four hours of hydrogen treatment caused a higher HE susceptibility in AH1 than in 20 hours charged AH2, but the highest HEI was measured from the longest charging. The results strongly indicate that the increased hydrogen charging time and higher strength properties achieved by longer age-hardening treatment causes severe HE in Inconel 718. [26]

5 Selective laser melted, and post-heat treated AISI 316 L steel

The microstructural features formed by six post-heat treatments, fracture mechanisms and mechanical properties were investigated after hydrogen charging to gain understanding of hydrogen embrittlement behavior from selective laser melted AISI 316 L steel. The most promising post-heat treatment for hydrogen environment is discussed and the candidates studied in the thesis are presented in Table 1. along with name abbreviations and treatment procedures.

Table 1. Post-heat treatments, name abbreviations and treatment procedures

Post-heat treatment	Abbreviation	Treatment procedure
Heat treatment	H1	At 1000 °C for 1 h [12]
Annealed	ANN	At 1100 °C for 1 h [6]
Hot isostatic pressing	HIP	At 1100 °C for 200 min in 103 MPa [6]
Hot isostatic pressing and cold working	CW	At 1100 °C for 200 min in 103 MPa + pre strained to 30 % elongation [6]
Heat treatment	H2	At 1066 °C for 1 h [23]
Heat treatment and polishing	HP	At 1066 °C for 1 h + polishing up to 3 µm [23]

5.1 The microstructural features

The main phase of AISI 316 L is austenite with columnar grains which was not affected by the SLM technique. The SLM as-built specimen exhibited cellular structure including high dislocation density with segregation to interdentritic regions and sub grains parallel to the building direction. Melt pools, un-melted particles, residual stress, microcracks and pores were common features observed, and the dendritic regions and dislocation cells were found to be overlapped. Chromium and molybdenum are ferrite stabilization elements leading to ferrite nucleation on the grain boundaries but the specimens did not contain these phases. [6,12,27]

The change from columnar to equiaxed grains was observed in H1, HIP, CW specimens due to the sufficient treatment temperature allowing recrystallization and growth of new grains which can be seen from Figure 2 [27]. On the contrary, columnar grain structure in ANN, H2 and HP specimens remained the same owing to the deficient post-heat treatment although, ANN was executed at 1100 °C and H2/HP at 1066 °C [6,23]. Similarities observed in all heat treatments were austenite microstructure, the absence of ferrite phases, deformation twinning and melt pool boundaries.

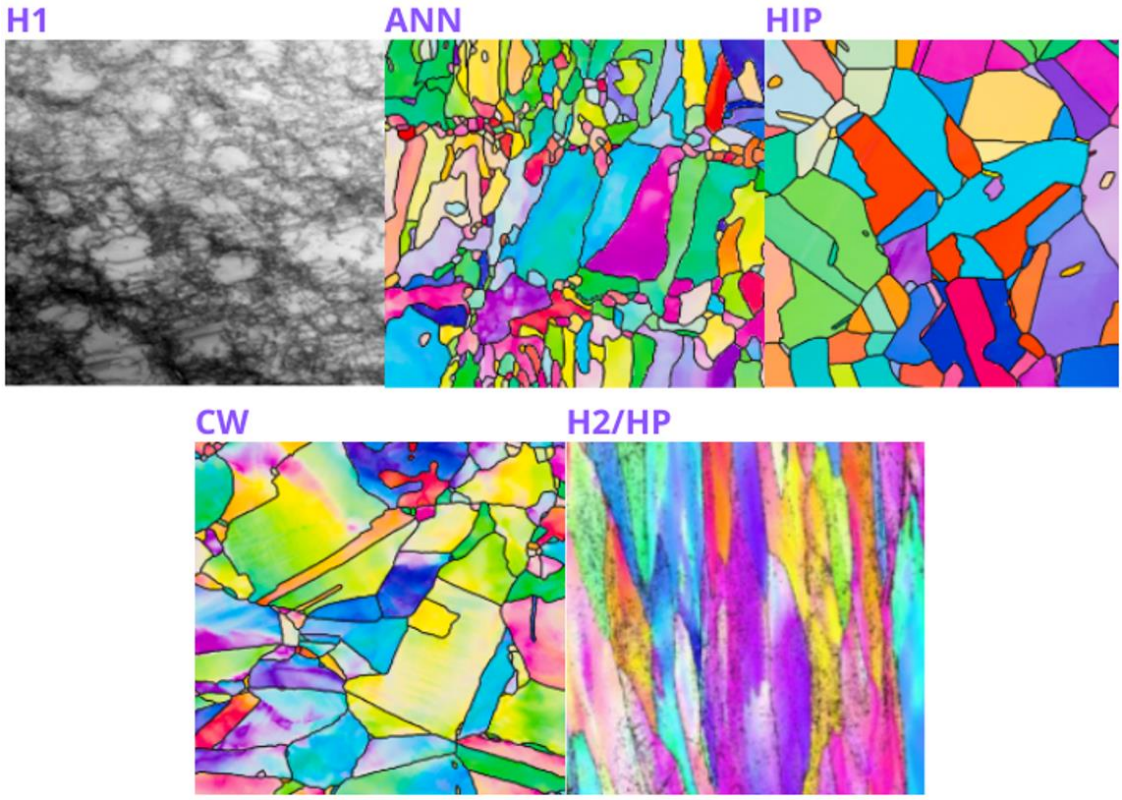

Figure 2. The microstructures of the post-heat treated AISI 316 L specimens [6,12,23]. Copyright 2021 Elsevier Ltd. [12]. Copyright 2023, Àlvarez et al. Published by Elsevier B.V. [6]. Copyright 2023, Hydrogen Energy Publications LLC. Published by Elsevier Ltd. [23]

Selective laser melted as-built specimen exhibited a high dislocation density which can be decreased by post-heat treatments and the mentioned phenomenon was noted in all specimens along with reduced in residual stresses. Even though, dislocation density was decreased after heat treatments the dislocation cells, precipitates and grain sizes were enlarged. The dislocation structure for H1, H2 and HP specimen was found to be disoriented and tangled meaning that specified cells or walls were not present. In contrast, similar dislocation structure was not mentioned for ANN, HIP and CW specimens but it was found that CW treatment formed disoriented structure in grain interiors caused by plastic deformation from pre-straining. [6,28]

When comparing post-heat treatments investigated, the microstructure of ANN specimen exhibited the most defects out of all including pores, microcracks and un-melted particles. The pores were formed by gas entrapment, un-melted particles were from defective process parameters and residual stresses lead to microcracks. Such defects were not present in the HIP or CW treated specimens excluding negligible sub-micrometer size porosity which was less than 1 μm^2 and 100 μm^2 in ANN specimen. The low porosity was also found in H1 and even in H2/HP specimens where the process parameters were chosen to minimize defect formation. [6,12,23]

5.2 The interaction between the microstructural features and hydrogen

After hydrogen charging, fracture surfaces of H1, H2 and HP remained ductile with micro void coalescence and were similar compared to non-charged counterparts. HIP specimen exhibited ductile fracture surface with few embrittle cleavage facets and interestingly, CW specimen which was HIP treated and pre-strained to 30 % elongation showed more brittle areas. What comes to ANN specimen, it was observed that increased hydrogen content enhanced the formation of embrittle cleavage facets. The void density of H1 specimen was increased at the fracture surface suggesting that voids were nucleated along the grain boundaries, slip-bands intersections, and precipitates. It must be pointed, that the changes in void formation may not directly influence on the mechanical properties which was noticed by debatable results while investigating void formation in the presence of hydrogen and its influence to elongation or reduction of area. [6,12,23]

Common deformation mechanisms in the presence of hydrogen leading to higher susceptibility to HE in AISI 316 L are stress concentrations at dislocation pileups around grain boundaries, strain-induced martensite formation, planar deformation, and deformation twinning. Martensite formation act as a fast diffusion path enhancing hydrogen accumulation in critical places promoting HAC [16]. However, the observed reduced dislocation density and defects along with the absence of other deformation mechanisms were discussed to be due to the initial dislocation morphology formed during SLM process followed by post-heat treatments [23]. Based on these observations, heat treated AISI 316 L has a high hydrogen embrittlement resistance and good potential for hydrogen environment applications.

In contrast to above mentioned, it is proven that the correlation between dislocation density and higher hydrogen embrittlement is not straightforward phenomenon because even if dislocation density is similar, the HE susceptibility can be higher. But increased dislocation mobility is proposed to be caused from hydrogen accumulation in the stress fields which can be furthermore transported through the lattice. These contradictory observations strongly indicate that the interplay between dislocation density, hydrogen concentration and hydrogen embrittlement susceptibility should be further examined. [12,23]

5.3 The mechanical properties

The mechanical properties were examined from each post-heat treated specimen prior and after hydrogen charging and the results are presented in Table 2. All studies did not measure every mechanical response and thus, all values are not available. As opposed to other specimens, the HEI values for H2 and HP were calculated by using elongation to fracture due to the lack of information on reduction of area and the rest were calculated by using RA values.

Table 2. The mechanical properties of the post-heat treated AISI 316 L specimens before and after hydrogen charging [6,12,23]

Post-heat treatment	Yield strength (MPa)	Tensile strength (MPa)	Reduction of area (%)	Elongation to fracture (%)
H1	388	611	67	57.5
H1 *	414	626	59	55.7
ANN	390	640	57	-
ANN *	425	680	55	-
HIP	300	610	59	-
HIP *	300	640	58	-
CW	700	780	56	-
CW *	750	810	49	-
H2	371	552	-	68.2
H2 *	412	596	-	67.4
HP	425	622	-	69.2
HP *	435	627	-	65.5

*Hydrogen charged specimen

The yield strength and tensile strength values remained the same or increased in all specimens after hydrogen charging due to a solid solution strengthening contribution obtained in the presence of hydrogen. Interesting finding between room and -50 °C temperature from ANN, HIP and CW examinations was that the HE susceptibility increased at -50 °C with the exception of HIP where it was decreased when tensile stress was parallel to the building direction [6]. As can be seen from Table 2. only the yield strength of HIP remained the same with the value being 300 MPa which was also, the lowest out of all specimens. RA and EF percentages decreased in all specimens after hydrogen charging but H1 and CW suffered the most reduction of area whereas only a little embrittlement was observed in other specimens. Based on this data, HEI values were calculated by using Equations 1. and 2. and are presented in Figure 3.

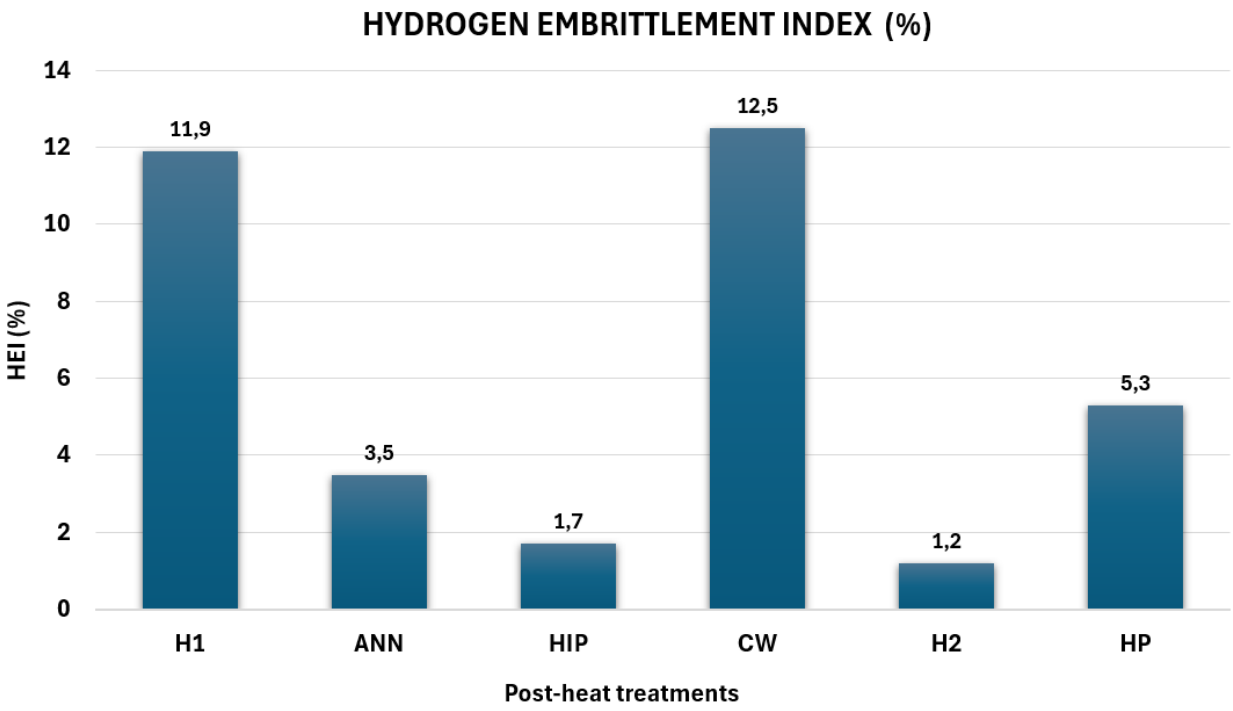

Figure 3. Hydrogen embrittlement index values of the post-heat treated AISI 316 L specimens [6,12,23]

Hydrogen assisted cracking has been suggested to clarify hydrogen embrittlement behavior of AISI 316 L steel in various conditions where hydrogen accumulation advances HELP and HEDE mechanisms causing HAC. The primary hydrogen diffusion paths proposed were martensitic structure and sub-grain/grain boundaries followed by proceeding to grain interiors when adequate diffusion rate is reached [29]. The decrease in dislocation density, residual stresses and the absence of martensite formation were in the key role of higher HE resistance when compared to the conventionally produced counterparts. Given the good HE resistance and the dominant ductile failure, the fracture mechanism was for the most part void nucleation and growth leading to coalescence and lastly, to fracture.

H2 and HP specimens were fabricated from the exact same material composition and the polishing treatment executed for HP was the only difference, yet the measured HEI values were 1.2 % for H2 and 5.3 % for HP. The divergence observed from these values can be explained by the absence of the polishing treatment in H2 specimen. The effect of the oxide layer to hydrogen permeation was examined and it was found to be lower when compared to surface processed counterparts. The remained oxide layer prevented hydrogen diffusion by acting as a barrier and decreased the possibility of HAC. In contrast, when AISI 310 was examined, it was found that rough surface increased lattice strains leading to higher hydrogen embrittlement and thus, the correlation between surface conditions and HE susceptibility is debatable needing

further investigation. H2 specimen had lower yield and tensile strengths than HP indicating that surface roughness did in fact negatively impact on these mechanical properties. Interestingly, the highest hydrogen embrittlement resistance was measured from H2 specimen which can be seen from the Figure 3. but it must be considered that this was calculated by using EF value. Also, the highest HEI was 12.5 % indicating that all calculated values were quite low. [23]

Pre-strained CW exhibited the most severe HE behaviour while HIP specimen treated the same had notable lower HEI value which was measured to be 1.7 %. One difference between these specimens were the pre-straining executed for CW which clearly affected to the mechanical properties. Despite that CW had greater vulnerability to HE, the yield and tensile strengths were higher than HIP treated specimen. As discussed earlier, internal stresses increment hydrogen embrittlement susceptibility by enhancing HELP mechanism and therefore, these results strongly suggests that the pre-straining is not suitable post-processing method. [6]

Tangled and disoriented dislocation structures observed from H1, H2 and HP specimens were proposed to improve HE resistance by suppressing interactions with hydrogen. Also, enlarged dislocation cells and grains observed in all specimens showed beneficial feature for HE behavior by lowering the influence of hydrogen. While these observations can partially explain the well hydrogen embrittlement resistance of AISI 316 L, it does not provide the explanation to the different HEI values because H1 had much higher value than H2 or HP. In addition, HIP and ANN treated counterparts indicated good HE resistance and above-mentioned dislocation structure was not mentioned in these specimens raising even more question marks on the subject. [12,23]

Based on the studies, the low porosity, precipitates or microcracks are not the primary hydrogen embrittlement contributor but initial dislocation structure and morphology. The observation can be supported by ANN specimen showing the most defects but still having good HE resistance with HEI value being 3.5 %. HIP and H2 indicated the least hydrogen embrittlement behaviour which is interesting because the specimens had very different microstructures gained from the heat treatments. Nevertheless, the low yield and tensile strengths of HIP must be considered when deciding possible applications and on the other hand, the rough surface with oxidation layer in H2 could be problematic in the place of use. The results point that examinations of the initial dislocation structure of HIP and H2/HP specimens and its impact to hydrogen embrittlement should be continued with keeping in mind that ANN treatment also showed potential HE resistance. Moreover, the equiaxed grain structure similar to HIP specimen could

be achieved in ANN specimen by modifying the process parameters of annealing treatment which gives a another intriguing research direction [6].

6 Selective laser melted, and post-heat treated Inconel 718 steel

In total, five post-heat treatments and their microstructural features, fracture surfaces, fracture mechanisms and mechanical properties were investigated to achieve an understanding of hydrogen embrittlement behavior of Inconel 718 steel. By modifying and combining heat treatments, the microstructural features can be altered leading to various mechanical properties. Thus, it is important to investigate the microstructural features formed during each post-heat treatment and the response to the mechanical properties with and without hydrogen. The examined post-heat treatments, name abbreviations and treatment procedures are presented in Table 3.

Table 3. The post-heat treatments, name abbreviations and treatment procedures

Post-heat treatment	Abbreviation	Treatment procedure
Solution treatment	ST	Solutioning at 1050 °C for 1 h + quenched in water [20]
Solution aging treatment	SAT	Solutioning at 1050 °C for 1 h + quenched in water + aging at 780 °C for 8 h [20]
Homogenization + double aging treatment	HA2	Stress relief at 1065 °C for 1.5 h + homogenization at 1066 °C for 1 h + first aging at 760 °C for 10 h + second aging at 649 °C for 8 h [14]
Direct aging	DA	Aging at 720 °C for 8 h + furnace cooled at the cooling rate of 50/h °C to at 620 °C and held 8 h + cooling to room temperature [7]
Homogenization + aging	HA1	Homogenization 1150 °C for 2 h + aging at 720 °C for 8 h + furnace cooled at the cooling rate of 50/h °C to at 620 °C and held 8 h + cooling to room temperature [7]

6.1 The microstructural features

Solidification substructure with Laves phases, notable number of dislocations and micro-segregation of Nb were detected on the cell walls in the as-built condition [21]. The grains were elongated to the building direction, melt pools were present and strain localized to the cellular structure walls. Mentioned features were formed owing to the high laser energy density and rapid cooling rate during the SLM process which can be detrimental to the material but, these can be supressed by post-heat treatments. The dislocation density was decreased in all heat treatments and the crucial strengthening γ' and γ'' phases were precipitated to the matrix by sufficient age-hardening treatment. The variety of microstructural features observed after post-heat treatments are summarized in Table 4. and discussed more closely. [30]

Table 4. The microstructural features observed after the post-heat treatments [7,14,20]

Post-heat treatment	Laves phase	γ′ and γ″ phases	δ phase	Complete recrystallization
ST	No	No	No	No
SAT	No	Yes	Yes	No
HA1	No	Yes	Yes	Yes
HA2	Yes	Yes	No	No
DA	Yes	Yes	Yes	No

In the as-built specimen, grains were elongated parallel to the building direction decreasing the mechanical properties when tensile stress was applied parallel to the elongated grains. Therefore, recrystallization was important to achieve by post-heat treatments but as it can be observed from Figure 4, the elongation remained in ST, SAT, HA2 or DA specimens indicating inadequate or nonexistent homogenization treatment time and temperature. 1-1.5 hours was not sufficient for the complete recrystallization and temperature lower than 1000 °C was not high enough causing the similar type of grain morphology than as-built specimen. On the contrary, two-hour homogenization at 1150 °C led to complete recrystallization in HA1 specimen suggesting good mechanical response. [7,14,20]

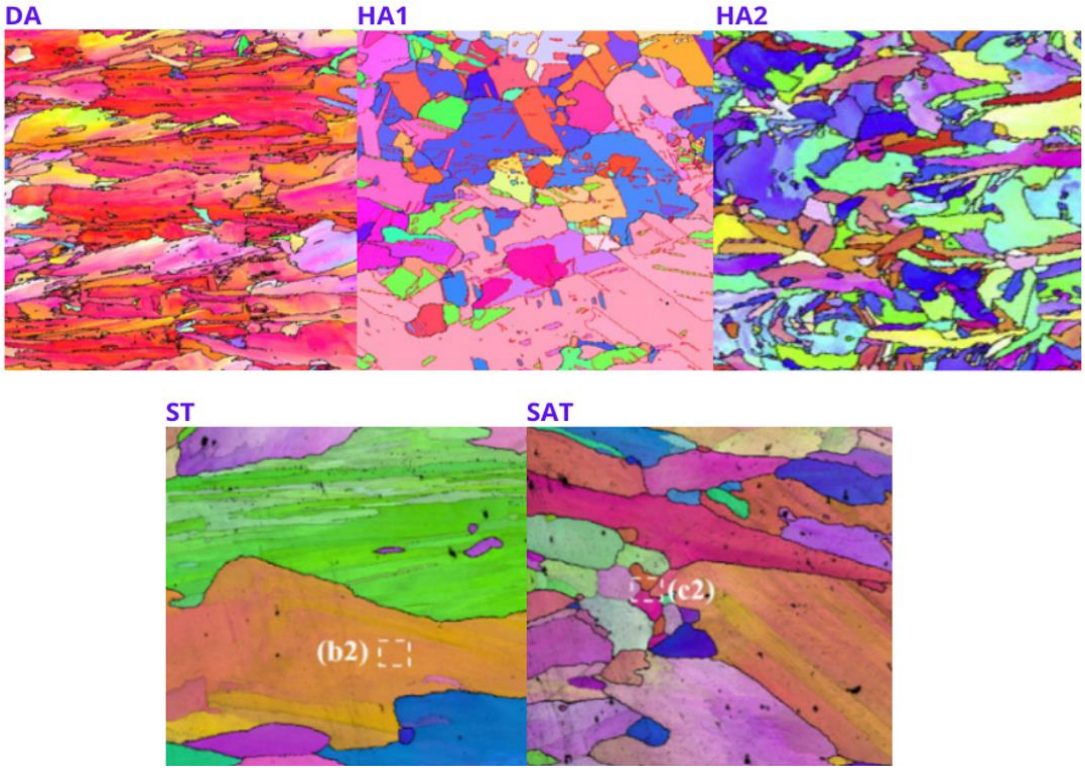

Figure 4. The microstructures of the post-heat treated Inconel 718 specimens [7,14,20]. Copyright 2023, Xu et al. Published by Elsevier B.V. [7]. Copyright 2022, 1 Acta Materialia Inc. Published by Elsevier Ltd. [14]. Copyright 2022, Yoo et al. Published by Elsevier Ltd. on behalf of Hydrogen Energy Publications LLC. [20]

As mentioned earlier, the γ′ and γ″ precipitates strengthens Inconel 718 which is why the adequate age-hardening treatment is inevitable processing stage for the steel. The strengthening γ′ and γ″ phases were not observed in the microstructure of ST specimen which can be explained by the absence of aging treatment [20]. In other specimens the aging stage allowed strengthening phases to precipitate in the grain interiors, mostly in cell boundaries of the cellular structure due to Nb and Ti segregation anticipating better mechanical properties when compared to ST specimen [7].

The dissolution of Laves phases varied between post-heat treatments depending on the time and temperature. It was reported in ST, SAT and HA1 examinations that the treatment temperature and time allowed Laves phases to dissolve into the matrix [20,21]. In contrast, HA2 treatment was not adequate for Laves phases to completely dissolve causing that these were observed at the high angle grain boundaries [14,20]. In a study investigating the dissolution of Laves phases, the examination was performed at 1150 °C with different treatment durations and it was found that the higher volume fraction of Laves phases dissolved with increasing treatment time. According to the study by Zhang et al, the lowest volume fraction was measured when homogenization time exceeded over 5 hours [31]. This observation is supported by HA2 treatment because the homogenization was executed at lower temperature for 1.5 hours leading to incomplete dissolution. However, the ST, SAT or HA1 specimens did not exhibit Laves phases leaving the dissolution behavior unclear. The lack of Laves phases in the lattice is crucial for improving hydrogen embrittlement resistance and thus, the dissolution behavior should be examined thoroughly. The DA treatment included only the aging stage leading that the dissolution was not occurred and the Laves phases remained clearly at the cell boundaries [7].

Contradictory results were also reported from the precipitation of δ phases. As it can be noticed from Table 4, the δ phases were not detected in ST or HA2 specimens but during HA1 and SAT treatments, those phases were formed along the grain boundaries [7,14,20]. What comes to the DA specimen, δ phases were observed mostly in the cell walls due to the insufficient dissolving temperature. Researchers proposed that the absence of δ phase in the HA2 specimen was caused by the high homogenization temperature because its solvus temperature is 1010 °C [14]. Nevertheless, δ phases were formed in HA1 and SAT specimens although the temperature exceeded 1010 °C indicating uncertainty of the precipitation behavior. As though Laves phases, δ phases are in an important role of HE which raises the importance to continue investigating the formation of these precipitants during heat treatments.

6.2 The effect of microstructural features on hydrogen trapping and fracture

Hydrogen changed the fracture mechanism of Inconel 718 from ductile to partial brittle and the embrittled area enlarged with increasing charging time indicating that higher concentration of hydrogen accumulated in the lattice enhances HE susceptibility [14]. HAC was caused by the combination of multiple microstructural features interacting with hydrogen leading to HE. Detected hydrogen assisted fracture mechanisms were hydrogen enhanced decohesion, hydrogen enhanced local plasticity and the interplay of both mechanisms. There were three crack propagation methods observed for Inconel 718 which were intergranular, transgranular and their combination. Frequently observed crack nucleation and propagation sites were grain boundaries and cell walls combined with Laves, δ, γ' and γ'' phases [17]. The grain boundaries acted as a hydrogen trapping sites and diffusion paths due to its large free volume [20]. The findings showed the complexity of hydrogen embrittlement because possible hydrogen accumulation sites and diffusion paths were several.

Hydrogen embrittlement behavior for solution treated and double aged specimen was investigated by fatigue crack propagation test and the fatigue crack growth rate (FGCR) was indeed increased in the presence of hydrogen. The sample in question showed 2.8 times higher acceleration of FGCR and it was reported that high hydrogen diffusion along grain boundaries and dislocation slip caused by HELP mechanism promoted IG cracking and decreased deformation expansion. In which case, decreased critical plastic strain for fatigue crack propagation promoted FCGR. Mentioned observation supports the theory that hydrogen reduces the ductility of Inconel 718 promoting hydrogen embrittlement behavior which was noted in all investigated specimens. [21]

During plastic deformation hydrogen atoms were carried via dislocations to regions with high dislocation density including slip lines or pile-ups near grain boundaries. It is suggested that the grain boundaries with increased dislocation density contain higher concentration of hydrogen causing improved crack nucleation and propagation susceptibility. The interaction between dislocations and hydrogen atoms promote HELP mechanism by enhancing slip localization which accumulates hydrogen and increases local strain at the grain boundaries, triple junctions and interfaces of δ phase causing intergranular HEDE [14]. Nonetheless, the dislocation density can be decreased by executing post-heat treatments and thus, are inevitable stages in the production of Inconel 718 steel. [7]

The Laves phases were found to be detrimental to materials mechanical properties after hydrogen charging because they acted as a fast diffusion path resulting increased concentration of diffusible hydrogen along the cell walls, grain boundaries and in the grain interiors. In addition, the interface of Laves phase and grain boundary was found as an accumulation site for hydrogen causing intergranular cracking along the grain boundaries. The Laves phases owns lower hydrogen diffusion coefficient than cell walls with higher dislocation density causing that the Laves phases can store more hydrogen. Based on these perceptions, the heat treatments which did not dissolve Laves phases completely had one more microstructural feature which can lead to hydrogen embrittlement. HA1, HA2 and DA treatments were not adequate for complete dissolution of Laves phases suggesting that these can have higher susceptibility to HE. [20]

The δ phases formed in the microstructure were found to be hydrogen trapping sites and were observed at grain boundaries or cell walls in SAT, HA1 and DA specimens causing cracking along the precipitant and the matrix. When specimen was under a tension, the interface was strained to a large extend resulting it to act as a trapping site for diffusible hydrogen which led to high accumulation in these regions [32]. High concentration of hydrogen in the interface of γ matrix and δ phase promoted HEDE mechanism along the grain boundaries leaving SAT, HA1 and DA specimens vulnerable for HE [7]. As well as other precipitants investigated, the Inconel 718 strengthening γ′ and γ″ phases enhanced hydrogen embrittlement by increasing high flow stress in the lattice. The combination of higher flow and grain boundary stresses promoted HAC which was observed from the SAT specimen. [20]

On the grounds of the observations made from each post-heat treatment, it can be stated that hydrogen embrittlement behavior was a combination of several microstructural features acting together. Suitable hydrogen accumulation and trapping sites were precipitants formed along the grain boundaries, cell walls and in the grain interiors. Absorbed and accumulated hydrogen in these regions advanced the hydrogen enhanced local plasticity and hydrogen enhanced decohesion leading to crack nucleation. Crack propagation methods found in Inconel 718 were intergranular, transgranular and the combination of both and the dominant fracture mechanism observed in all specimens was HELP followed by HEDE mechanism. However, thorough understanding of the relationship between microstructural features and hydrogen embrittlement cannot be achieved by current research data which raises the necessity for further studies.

6.3 The mechanical properties

The mechanical properties were examined prior and post hydrogen charging and the results of each post-heat treated specimen are presented in Table 5. The yield strength was not notable affected by hydrogen in any specimen but for one's part, a slight decrease was observed on tensile strength values, especially in ST and DA. The decrease in these specimens can be explained by the absence of γ' and γ'' precipitants in ST and the lack of solution/homogenization treatment in DA [7,20]. The measured yield and tensile strengths of ST were 550 MPa and 679 MPa which were notable lower when compared to other specimens. The difference was caused by the absence of age-hardening stage preventing the strengthening γ' and γ'' phases to form into the matrix. In addition, the loss of elongation after hydrogen charging was prominent (from 41 to 12 %) indicating that ST post-heat treatment is not suitable for Inconel 718 when material is exposed to hydrogen environment. It must be added that the yield and tensile strength values are also low without hydrogen and thus, the treatment is not appropriate option even for non-hydrogen environment.

Table 5. Slow strain tensile test results of the post-heat treated Inconel 718 specimens prior and post hydrogen charging [7,14,20]

Post-heat treatment	Yield strength (MPa)	Tensile strength (MPa)	Elongation to fracture (%)
ST	550	904	41
ST *	550	679	12
SAT	1110	1357	22.5
SAT *	1110	1154	7
HA1	1215	1250	14
HA1 *	1215	1210	9
HA2	1222	1396	15.2
HA2 *	1231	1354	7.6
DA	1098	1400	7
DA *	1098	1100	3

*Hydrogen charged specimen

Interestingly, the decrease of EF values occurred in all hydrogenated specimens which shows severe weakening in ductility and increased HE susceptibility. HEI percentages were calculated by using Equation 1. where elongation values are taken into a consideration and the results are presented in Figure 5. Incomplete recrystallization, Laves, δ and γ' and γ'' phases caused by the aging treatment led to the highest strength prior the hydrogen charging in DA specimen.

However, the downside of DA treatment was the increased HE susceptibility due to the plenty of precipitates in the matrix, high strength formed by the aging treatment and the lack of solutioning/homogenization treatment. HEI value calculated for DA specimen was 57.1 % and 50 % for HA2 which also exhibited incomplete recrystallization, Laves and γ′ and γ″ phases. Basing on the HEI values, neither of those specimens is the best choice for hydrogen environment but also, neither showed the highest HE vulnerability.

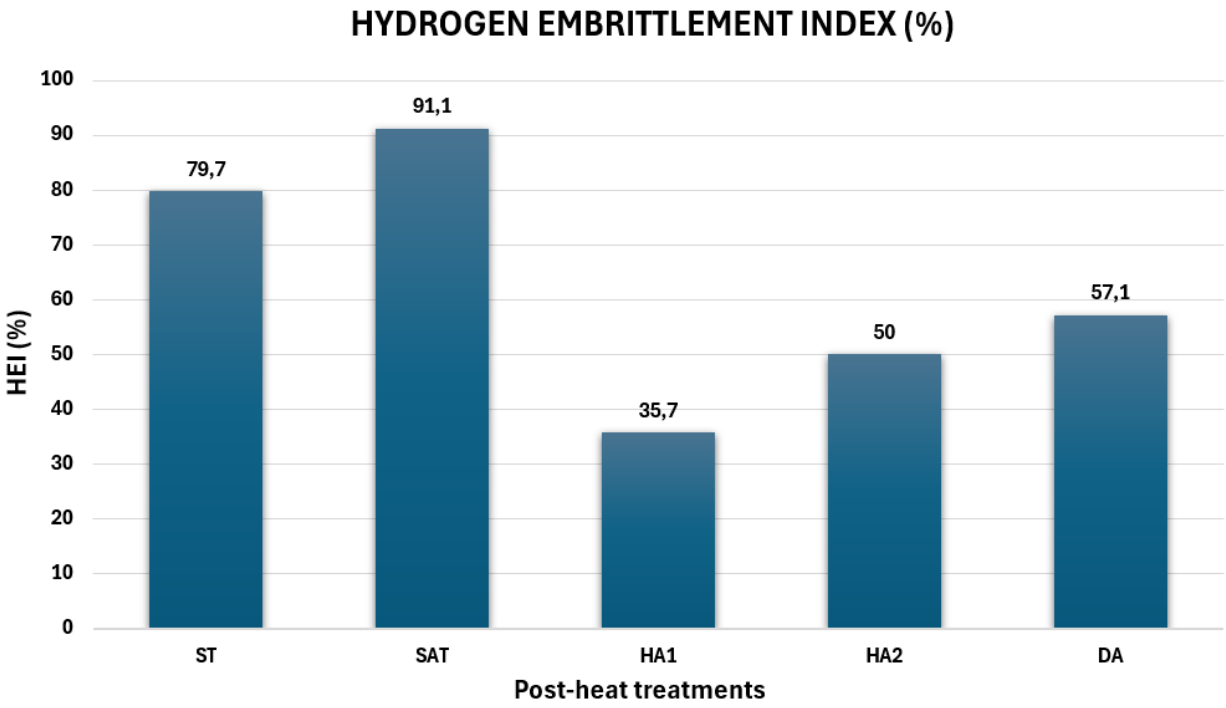

Figure 5. Hydrogen embrittlement index values of the post-heat treated Inconel 718 specimens [7,14,20]

The most severe hydrogen embrittlement behavior was discovered from SAT treatment with HEI value being 91.1 % while the highest HE resistance was detected from HA1 specimen where the HEI value was 35.7 %. Interestingly, both specimens had δ, γ′ and γ″ phases and no Laves phases but the HE behavior differed considerably. The difference may be caused from to the amount of δ phase precipitated along the grain boundaries, as there were only a few of these precipitates in HA1 specimen. Moreover, the homogenization treatment in HA1 was sufficient for homogeneous distribution of γ′ and γ″ phases and for complete recrystallization. These factors acting together decreased the hydrogen embrittlement susceptibility and made HA1 the most compatible post-heat treatment for Inconel 718 when steel is exposed to hydrogen environment. [7]

7 Conclusions

Regardless of several studies executed throughout the years, hydrogen embrittlement has remained debatable, but it seems that HE behaviour in AISI 316 L and Inconel 718 steels is an interplay of multiple microstructural features enhancing HELP and HEDE mechanisms. However, the primary hydrogen embrittlement factors were separate where, the focus in Inconel 718 is the synergia of precipitants γ', γ'', δ and Laves phases and in AISI 316 L the dislocation structure and density. One resemblance in both steels was that the grain boundaries and cell walls are vulnerable for hydrogen accumulation, crack nucleation and propagation. Figure 6. clearly indicates that the highest hydrogen embrittlement susceptibility was discovered from the conventionally fabricated Inconel 718 even though, Laves phases were absent.

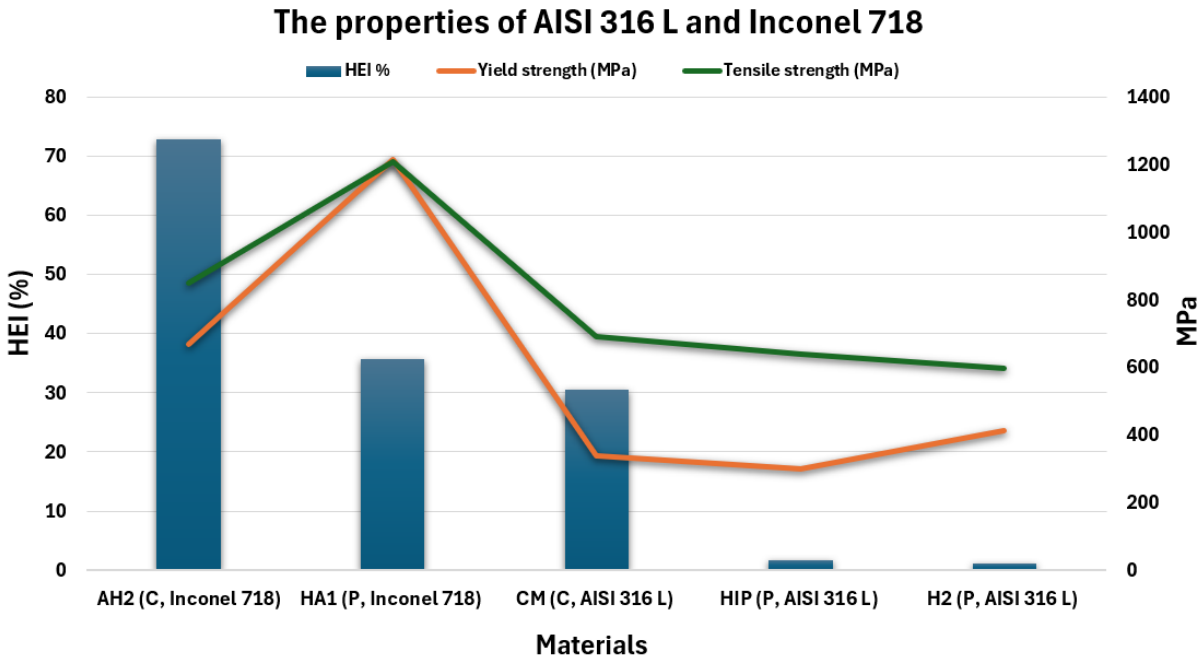

Figure 6. HEI (bars, left axis), yield and tensile strength (lines, right axis) values of the post-heat treated AISI 316 L and Inconel 718 steels that exhibited the highest resistance to hydrogen embrittlement. C indicates conventionally manufactured specimens and P selective laser melted counterparts. [6,7,12,14,20,23]

The selective laser melting technique improved the HE resistance in both steels when compared to conventionally produced counterparts and the increased hydrogen environment compatibility is proposed to be due to the unique microstructure formed during SLM process. Hydrogen embrittlement susceptibility of SLM Inconel 718 was 35.7 % and was prominently higher than in SLM or conventionally manufactured AISI 316 L which were measured to be less than 2 % and 30.5 %. The decrease in ductility was considerable in Inconel 718 while only a slight in AISI 316 L leading to completely different HEI values. The yield or tensile strength values

were not notable affected in the presence of hydrogen but are higher in Inconel 718. The highest HE resistance in Inconel 718 was achieved by the homogenization plus aging treatment (HA1) and the best performance of AISI 316 L was obtained by the heat treatment without polishing (H2) and the hot isotopic pressing (HIP) with minimal hydrogen embrittlement behaviour. Based on the HEI, yield and tensile strength values summarized in the Figure 6, the correlation between high strength properties and increased HE susceptibility is clear.

Although, two heat treatments executed for AISI 316 L indicated superior compatibility for hydrogen environment the yield and tensile strengths of HIP and H2 were low and may be insufficient in the application. Moreover, H2 treatment resulted better mechanical properties but did not compare with Inconel 718 and, this post-heat treatment did not include surface polishing which may be problematic in the place of use. After careful consideration, the HIP treated AISI 316 L could be the first choice of steel for hydrogen environment when yield or tensile strengths are not required to be higher than the measured values. However, if these mechanical properties of AISI 316 L are inadequate, HA1 treated Inconel 718 is a potential option.

References

[1] C. Scott, Wohlers Report 2023 Unveils Continued Double-Digit Growth, Wohlers Assoc. (2023). https://wohlersassociates.com/news/wohlers-report-2023-unveils-continued-double-digit-growth/ (accessed February 12, 2024).

[2] Special Metals - Search Results, (n.d.). https://www.specialmetals.com/search-results.html?sisea_offset=5&search=inconel+718+ (accessed March 30, 2024).

[3] Kemiallinen analyysi, Valbruna Nord. Oy (n.d.). https://valbruna.fi/portfolio/kemiallinen-analyysi (accessed April 1, 2024).

[4] S. Bruschi, E. Simonetto, M. Pigato, A. Ghiotti, R. Bertolini, Analysis of the AISI 316 stainless steel sheet response to sub-zero deformation temperatures, Manuf. Lett. 35 (2023) 208–214. https://doi.org/10.1016/j.mfglet.2023.08.023.

[5] G.H. Lee, M. Park, B. Kim, J.B. Jeon, S. Noh, B.J. Kim, Evaluation of precipitation phase and mechanical properties according to aging heat treatment temperature of Inconel 718, J. Mater. Res. Technol. 27 (2023) 4157–4168. https://doi.org/10.1016/j.jmrt.2023.10.196.

[6] G. Álvarez, Z. Harris, K. Wada, C. Rodríguez, E. Martínez-Pañeda, Hydrogen embrittlement susceptibility of additively manufactured 316L stainless steel: Influence of post-processing, printing direction, temperature and pre-straining, Addit. Manuf. 78 (2023) 103834. https://doi.org/10.1016/j.addma.2023.103834.

[7] D.-H. Lee, Y. Zhao, S.Y. Lee, D. Ponge, E.A. Jägle, Hydrogen-assisted failure in Inconel 718 fabricated by laser powder bed fusion: The role of solidification substructure in the embrittlement, Scr. Mater. 207 (2022) 114308. https://doi.org/10.1016/j.scriptamat.2021.114308.

[8] Kh. Moeinfar, F. Khodabakhshi, S.F. Kashani-bozorg, M. Mohammadi, A.P. Gerlich, A review on metallurgical aspects of laser additive manufacturing (LAM): Stainless steels, nickel superalloys, and titanium alloys, J. Mater. Res. Technol. 16 (2022) 1029–1068. https://doi.org/10.1016/j.jmrt.2021.12.039.

[9] W. Wang, S. Wang, X. Zhang, F. Chen, Y. Xu, Y. Tian, Process parameter optimization for selective laser melting of Inconel 718 superalloy and the effects of subsequent heat treatment on the microstructural evolution and mechanical properties, J. Manuf. Process. 64 (2021) 530–543. https://doi.org/10.1016/j.jmapro.2021.02.004.

[10] E. Liverani, S. Toschi, L. Ceschini, A. Fortunato, Effect of selective laser melting (SLM) process parameters on microstructure and mechanical properties of 316L austenitic stainless steel, J. Mater. Process. Technol. 249 (2017) 255–263. https://doi.org/10.1016/j.jmatprotec.2017.05.042.

[11] J. Gunasekaran, P. Sevvel, I. John Solomon, Metallic materials fabrication by selective laser melting: A review, Mater. Today Proc. 37 (2021) 252–256. https://doi.org/10.1016/j.matpr.2020.05.162.

[12] K.M. Bertsch, A. Nagao, B. Rankouhi, B. Kuehl, D.J. Thoma, Hydrogen embrittlement of additively manufactured austenitic stainless steel 316 L, Corros. Sci. 192 (2021) 109790. https://doi.org/10.1016/j.corsci.2021.109790.

[13] P. Metalnikov, G. Ben-Hamu, D. Eliezer, Hydrogen Trapping in Laser Powder Bed Fusion 316L Stainless Steel, Metals 12 (2022) 1748. https://doi.org/10.3390/met12101748.

[14] J. Yoo, S. Kim, M.C. Jo, H. Park, J.E. Jung, J. Do, D.W. Yun, I.S. Kim, B.-G. Choi, Investigation of hydrogen embrittlement properties of Ni-based alloy 718 fabricated via laser powder bed fusion, Int. J. Hydrog. Energy 47 (2022) 18892–18910. https://doi.org/10.1016/j.ijhydene.2022.04.045.

[15] S. Liang, M. Huang, L. Zhao, Y. Zhu, Z. Li, Effect of multiple hydrogen embrittlement mechanisms on crack propagation behavior of FCC metals: Competition vs. synergy, Int. J. Plast. 143 (2021) 103023. https://doi.org/10.1016/j.ijplas.2021.103023.
[16] J. Yao, Q. Tan, J. Venezuela, A. Atrens, M.-X. Zhang, Recent research progress in hydrogen embrittlement of additively manufactured metals – A review, Curr. Opin. Solid State Mater. Sci. 27 (2023) 101106. https://doi.org/10.1016/j.cossms.2023.101106.
[17] J. Sanchez, A. Ridruejo, P.L. De Andres, Diffusion and trapping of hydrogen in carbon steel at different temperatures, Theor. Appl. Fract. Mech. 110 (2020) 102803. https://doi.org/10.1016/j.tafmec.2020.102803.
[18] S.K. Dwivedi, M. Vishwakarma, Hydrogen embrittlement in different materials: A review, Int. J. Hydrog. Energy 43 (2018) 21603–21616. https://doi.org/10.1016/j.ijhydene.2018.09.201.
[19] J. Song, W.A. Curtin, A nanoscale mechanism of hydrogen embrittlement in metals, Acta Mater. 59 (2011) 1557–1569. https://doi.org/10.1016/j.actamat.2010.11.019.
[20] J. Xu, Z. Hao, Z. Fu, X. He, H. Wang, G. Xu, Hydrogen embrittlement behavior of selective laser-melted Inconel 718 alloy, J. Mater. Res. Technol. 23 (2023) 359–369. https://doi.org/10.1016/j.jmrt.2022.12.196.
[21] Z. Fu, P. Wu, Q. Yang, Q. Kan, G. Kang, Hydrogen-assisted fatigue crack propagation behavior of selective laser–melted Inconel 718 alloy, Corros. Sci. 227 (2024) 111745. https://doi.org/10.1016/j.corsci.2023.111745.
[22] F. Ye, T. Zhu, K. Mori, Q. Xu, Y. Song, Q. Wang, R. Yu, B. Wang, X. Cao, Effects of dislocations and hydrogen concentration on hydrogen embrittlement of austenitic 316 stainless steels, J. Alloys Compd. 876 (2021) 160134. https://doi.org/10.1016/j.jallcom.2021.160134.
[23] L. Claeys, L. Deconinck, K. Verbeken, T. Depover, Effect of additive manufacturing and subsequent heat and/or surface treatment on the hydrogen embrittlement sensitivity of 316L austenitic stainless steel, Int. J. Hydrog. Energy 48 (2023) 36142–36157. https://doi.org/10.1016/j.ijhydene.2023.05.215.
[24] J. Park, T.T. Nguyen, H.M. Heo, U.B. Baek, Hydrogen-related with the change in mechanical properties and deformation behavior of 316 L austenite stainless steel, Mater. Charact. 197 (2023) 112666. https://doi.org/10.1016/j.matchar.2023.112666.
[25] Z. Tarzimoghadam, D. Ponge, J. Klöwer, D. Raabe, Hydrogen-assisted failure in Ni-based superalloy 718 studied under in situ hydrogen charging: The role of localized deformation in crack propagation, Acta Mater. 128 (2017) 365–374. https://doi.org/10.1016/j.actamat.2017.02.059.
[26] X. Lu, D. Wang, D. Wan, Z.B. Zhang, N. Kheradmand, A. Barnoush, Effect of electrochemical charging on the hydrogen embrittlement susceptibility of alloy 718, Acta Mater. 179 (2019) 36–48. https://doi.org/10.1016/j.actamat.2019.08.020.
[27] J. Bedmar, S. García-Rodríguez, M. Roldán, B. Torres, J. Rams, Effects of the heat treatment on the microstructure and corrosion behavior of 316 L stainless steel manufactured by Laser Powder Bed Fusion, Corros. Sci. 209 (2022) 110777. https://doi.org/10.1016/j.corsci.2022.110777.
[28] Q. Chao, S. Thomas, N. Birbilis, P. Cizek, P.D. Hodgson, D. Fabijanic, The effect of post-processing heat treatment on the microstructure, residual stress and mechanical properties of selective laser melted 316L stainless steel, Mater. Sci. Eng. A 821 (2021) 141611. https://doi.org/10.1016/j.msea.2021.141611.
[29] J. Lin, F. Chen, F. Liu, D. Xu, J. Gao, X. Tang, Hydrogen permeation behavior and hydrogen-induced defects in 316L stainless steels manufactured by additive manufacturing, Mater. Chem. Phys. 250 (2020) 123038. https://doi.org/10.1016/j.matchemphys.2020.123038.

[30] L. Zhou, A. Mehta, B. McWilliams, K. Cho, Y. Sohn, Microstructure, precipitates and mechanical properties of powder bed fused inconel 718 before and after heat treatment, J. Mater. Sci. Technol. 35 (2019) 1153–1164. https://doi.org/10.1016/j.jmst.2018.12.006.
[31] S. Zhang, L. Wang, X. Lin, H. Yang, W. Huang, The formation and dissolution mechanisms of Laves phase in Inconel 718 fabricated by selective laser melting compared to directed energy deposition and cast, Compos. Part B Eng. 239 (2022) 109994. https://doi.org/10.1016/j.compositesb.2022.109994.
[32] L. Liu, C. Zhai, C. Lu, W. Ding, A. Hirose, K.F. Kobayashi, Study of the effect of δ phase on hydrogen embrittlement of Inconel 718 by notch tensile tests, Corros. Sci. 47 (2005) 355–367. https://doi.org/10.1016/j.corsci.2004.06.008.